EPJ Web of Conferences **6**, 37002 (2010)
DOI:10.1051/epjconf/20100637002

Viscoelastic material properties' identification using high speed full field measurements on vibrating plates

A. Giraudeau[1,a] and F. Pierron[2]

[1] L.M.P.F. Arts et Metiers ParisTech, BP 508, 51006 Châlons en Champagne, France
[2] L.M.P.F. Arts et Metiers ParisTech, BP 508, 51006 Châlons en Champagne, France

Abstract. The paper presents an experimental application of a method leading to the identification of the elastic and damping material properties of isotropic vibrating plates. The theory assumes that the searched parameters can be extracted from curvature and deflection fields measured on the whole surface of the plate at two particular instants of the vibrating motion. The experimental application consists in an original excitation fixture, a particular adaptation of an optical full-field measurement technique, a data preprocessing giving the curvature and deflection fields and finally in the identification process using the Virtual Fields Method (VFM). The principle of the deflectometry technique used for the measurements is presented. First results of identification on an acrylic plate are presented and compared to reference values. Details about a new experimental arrangement, currently in progress, is presented. It uses a high speed digital camera to over sample the full-field measurements.

1 Introduction

The measurement of material elastic stiffness and damping parameters, essential for the prediction of the vibrating or vibro-acoustic behaviour of a large range of structures, is common in material testing laboratories. The identification of the stiffness parameters is usually performed using tension, bending or torsion tests on rectangular coupons leading to simple stress states that can be expressed as functions of the specimen geometry and the applied load through a closed-form solution of the mechanical problem. Nevertheless, these procedures exhibit certain drawbacks. First, experimental boundary conditions must comply with that of the mechanical model, which is not always easy to achieve. Then, only a small number of parameters can be retrieved from a specific test because of the very simple stress state. As a result, several tests have usually to be performed to identify the full set of material parameters, increasing the cost of the procedure. As an alternative, several authors have tried to use the resonance frequencies of bending plates to identify the full stiffness tensor. More recently, the above approach was refined by using not only modal frequencies but also mode shapes. An alternative to these methods was suggested by Grédiac et al. [1] making use of the measurement of slope fields at the surface of bent plates and performing the identification through a particular application of the principle of virtual work, so-called Virtual Fields Method (VFM). This procedure uses the global equilibrium of the observed part of the coupon. One advantage of this technique is that stiffnesses are obtained directly (no iterations, no optimization scheme) and that restrictions on specimen geometry and boundary conditions are less critical than with other methods. The measurement of damping parameters is a more complex problem than stiffness because of all the parasitic dissipation that is usually added in a classical mechanical test. One another main advantage of the present extension of this method is to greatly minimize the parasitic effects of the boundary conditions.

[a] e-mail: alain.giraudeau@chalons.ensam.fr

2 Theory - Virtual Fields Method (V.F.M.)

2.1 Considered case

The considered coupon of the isotropic tested material is a rectangular thin plate (thickness h), free on its external boundary and clamped to an excitation device which imposes a sine driving movement in the out-of-plane direction (inertial excitation). The external boundary of the plate is free. Assuming linear viscoelastic behaviour of the material and thin plate theory, the vibrating response of the plate is pure harmonic bending at the same frequency [2], [3]. This response can be described by the actual deflection field $w(x, y, t)$ such that:

$$w(x, y, t) = \overline{w}(x, y) \cdot \cos(\omega t + \phi(x, y)) \tag{1}$$

or using complex notation:

$$w(x, y, t) = Re\Big\{[w_r(x, y) + jw_i(x, y)] \cdot \exp(j\omega t)\Big\} \tag{2}$$

2.2 Global equilibrium

The plate can be virtually divided in two parts: a small zone called Π surrounding the clamping area and the second part Ω which is free on its external boundary. The virtual border between these two parts Π and Ω shall be called Γ. In the case of small perturbations, the local equation of equilibrium can be written at any point M of Ω:

$$\sigma_{ij,j} + f_i = \rho \cdot \gamma_i \tag{3}$$

Each term could be multiplied by a u^* function which is user selected and must be continuous over Ω. This function can be seen as a displacement field which is virtually imposes all over Ω:

$$\sigma_{ij,j} \cdot u^* + f_i \cdot u^* = \rho \cdot \gamma_i \cdot u^* \tag{4}$$

Equation 4 could then be integrated over Ω and leads to:

$$\int_\Omega \sigma_{ij,j} \cdot u^* \cdot dV + \int_\Omega f_i \cdot u^* \cdot dV = \int_\Omega \rho \cdot \gamma_i \cdot u^* \cdot dV \tag{5}$$

Using the divergence theorem for the calculation of the first term and assuming ε^* is the virtual strain field related to the virtual displacement field u^*, Eq. 5 can be rearranged in a more useful expression:

$$-\int_\Omega \sigma : \epsilon^* \cdot dV + \int_{\partial\Omega} T_i \cdot u^* \cdot dS + \int_\Omega f_i \cdot u^* \cdot dV = \int_\Omega \rho \cdot \gamma_i \cdot u^* \cdot dV \tag{6}$$

It can be seen each term of Eq. 6 could be viewed as a virtual work under the action of the virtual displacement u^* and the related virtual strain. Respectively from the left to the right one can find, the virtual work of the internal forces, of the junction forces along the Γ border, of the volume forces and finally of the acceleration forces. Due to the assumption of the linear behaviour of the plate material, the acceleration of the harmonic response field of the plate can be simply expressed as $\gamma_i = \omega^2 \cdot u_i$. Finally assuming that the volume forces can be neglected, the global equilibrium of the part Ω free along its external boundary, can be written:

$$-\int_\Omega \sigma : \epsilon^* \cdot dV + \int_\Gamma T \cdot u^* \cdot dS = -\rho\omega^2 \int_\Omega w \cdot u^* \cdot dV \tag{7}$$

2.3 Virtual Fields Method (V.F.M.)

The principle of the virtual field method is to replace the stress components in the above equation by the actual elastic strains through the constitutive equations which parameters are to be identified. Then, by selecting 'appropriate' virtual fields, $u^*(x, y)$, it is possible to derive equations relating the materials constitutive parameters to integral functions of the actual strains. In the present case, the only external forces acting on Ω are the connection forces on the Γ border. If a virtual displacement field u^* is selected such that it cancels the virtual work of these connection forces then the second term of Eq. 7 is null and only the first and the last integrals of the latter remain. It can be shown that the first term can be expressed according to the Love-Kirchhoff theory. Then Eq. 7 can be rewritten as:

$$-\int_S \langle \kappa^* \rangle \cdot [D + j\omega B] \cdot \{\kappa\} \cdot dS = -\rho\,\omega^2 \int_S \langle w^* \rangle \cdot \{w\} \cdot dS \tag{8}$$

where $\{w\}$ and $\{\kappa\}$ are the actual deflection and curvatures fields to be measured on the surface S of Ω whereas $\langle w^* \rangle$ and the corresponding $\langle \kappa^* \rangle$ are the virtual deflection and curvatures fields to be selected for the identification. $[D]$ and $[B]$ are respectively the isotropic bending stiffness and viscous damping matrices, whose D_{xx}, D_{xy}, B_{xx} and B_{xy} components are the unknown materials parameters. It must be pointed out that this relationship is valid whatever the excitation frequency, at resonance or out of resonance.
By separating the real and imaginary parts of Eq. 8 it can be shown that the latter can be split into two independent ones, presented in Eq. 9:

$$\begin{aligned} D_{xx} \cdot G_r + D_{xy} \cdot H_r - \omega B_{xx} \cdot G_i - \omega B_{xy} \cdot H_i &= \rho\, h\, \omega^2 \int_S w_r \cdot w^*\, dS \\ D_{xx} \cdot G_r + D_{xy} \cdot H_r - \omega B_{xx} \cdot G_i - \omega B_{xy} \cdot H_i &= \rho\, h\, \omega^2 \int_S w_r \cdot w^*\, dS \end{aligned} \tag{9}$$

where G_p and H_p denotes combinations of products between virtual and actual curvatures such :

$$G_p = \int_S (\kappa_x^p \kappa_x^* + \kappa_y^p \kappa_y^* + \frac{1}{2}\kappa_s^p \kappa_s^*)\, dS \qquad ; \qquad H_p = \int_S (\kappa_y^p \kappa_x^* + \kappa_x^p \kappa_y^* - \frac{1}{2}\kappa_s^p \kappa_s^*)\, dS \tag{10}$$

These quantities are computed using the real or imaginary parts of the actual curvature fields according to whether the p index is r or i.

2.4 Virtual fields selection

The selection of the virtual fields is a major task of the identification method. It is carried out using three successive criteria:

- First, using piecewise virtual fields [4], virtual deflection and curvature fields are generated such that they are null along the Γ border leading to the cancelation of the virtual work of the connection forces;
- Then, to ensure independence between the four equations issued from Eq. 9, a particular application of a work by Grédiac et al [5] is used to select the 'special' virtual deflection fields $w^*_{(1)}$, $w^*_{(2)}$ which verify particular values of G_p and H_p and lead to very simple calculations of the parameters;
- The final selection is achieved using an adaptation of the work by Avril et al [6] providing 'optimized' virtual fields which minimize the effects of the measurement noise on the identification results.

3 Experimental

3.1 Presentation

As presented in the previous section, the application of the Virtual Fields Method to the present case requires an excitation arrangement providing an inertial out-of-plane excitation of the plate which is

free at its boundaries and a measurement set-up based on an optical method providing the curvature fields and the out-of-plane displacement fields on the whole surface of the plate. These measurements must be taken at two particular times: in-phase and at $\pi/2$ lag with the driving movement of the plate. These two particular positions correspond respectively to the real and imaginary part of the displacement field of the coupon. Tests have been carried out using an acrylic $200 \times 160 \times 3mm^3$ specimen. The sine out of plane inertial excitation is provided by a dedicated device where the coupon is clamped in its center between the end of the driving rod of the device and a rigid steel washer of the same diameter, tightened by an axial screw. An accelerometer mounted on the rod is used to control the imposed driving movement

3.2 Slope field measurements by deflectometry

To avoid noise problems on curvatures arising from a double spatial differentiation of the measured deflection fields, measurement of the slope field is preferred through deflectometry [7,8] which is a non interferometric technique in white light. A cross line grating (grid) is placed in front of the tested plate which must have a mirror like reflective surface. The image of the grid on the surface of the plate is observed with a digital camera. When the plate bends (under the effect of static or dynamic loads), the main detected phenomenon is the variation of the local slope of the plate. When the plate is deformed, the ray reflected by point M, that will be seen by a given pixel of the camera detector, comes from point Q slightly shifted with respect to point P from where the ray comes when the plate is undeformed or in a previous deformed state (see Fig. 1).

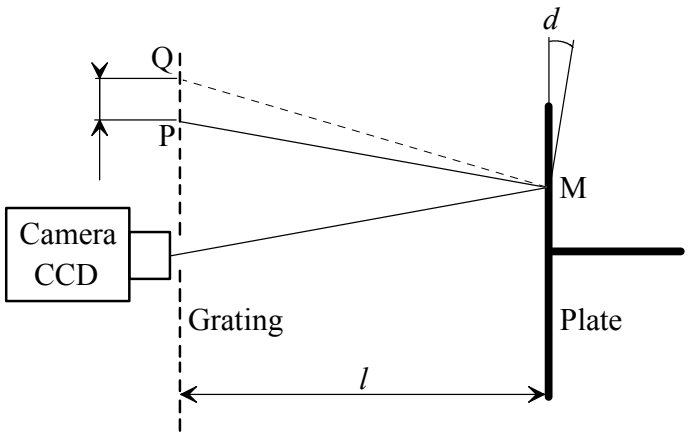

Fig. 1. Deflectometry principle

If the local slope varies by $d\alpha$ the apparent displacement of the image of the grating will be $\delta = 2l$ where l is the distance between the grid and the plate ($850mm$ in the present case). The reference grid serves as a ruler and its images are analyzed using spatial phase-stepping ("Windowed Discrete Fourier Transform" algorithm) which enables a refined evaluation of the spatial phase of the reflected light. Using a pre-processing to separate the information in the two in-plane orthogonal directions of the grid, the two components of slope fields can be measured simultaneously. It can be shown that the sensitivity derives directly from pure geometrical considerations and is very close to 5.5 radians of spatial phase variation per milliradian of slope variation and through and experimental estimation of the measurement noise, it can be shown that the slope resolution is about $4nm$ per mm. In the initial experimental arrangement, image freezing is achieved using a flash triggered by the driving movement with a 0 or $\pi/2$ lag to get the images respectively related to the real or imaginary parts of the response.

Deflection and curvature fields are respectively issued from numerical integration and differentiation of polynomial fittings of the slope fields.

3.3 Identification results

Identification have been carried out using Eq. 9 with a set of two displacement virtual fields selected such they are null along the rectangular border Γ of the Ω zone surrounding the clamping area. The two stiffness parameters D_{xx}, D_{xy} and the two viscous damping parameters B_{xx}, B_{xy} of the tested material are first extracted. According to [9] material elastic properties, Young modulus E and Poisson ratio ν and their related loss factors $\eta = tan(\delta)$ and η_ν are presented in Table 1 below for five excitation frequencies. It must be noticed that the 100 Hz excitation is close to a resonance of the tested plate and the four other frequencies are out of resonance. The identified values can be compared with the Young modulus and its loss factor issued from DMTA tests and vibrating tests performed by the authors in the same frequency range on beam specimens. The showed values of the material properties and their relative coefficients of variation issued are from eight measurements on each tested frequencies.

Table 1. Experimentally identified engineering constants and loss factors.

Frequency	(Hz)	70	80	90	100	110	Beams
E	Mean	4.62	4.63	4.70	4.55	4.69	4.9
(GPa)	Coeff. Var. (%)	1.8	1.3	1.2	0.8	0.6	2.4
ν	Mean	0.33	0.33	0.3	0.34	0.34	
	Coeff. Var. (%)	1.3	0.5	0.8	0.6	0.6	
$\tan(\delta)$	Mean	0.065	0.052	0.050	0.064	0.062	0.054
	Coeff. Var. (%)	2.9	1.8	1.8	1.9	1.1	3.5
η_ν	Mean.	0.024	0.013	0.014	0.031	0.022	
	Coeff. Var. (%)	10.3	4.7	6.0	9.1	7.1	

The results for the elastic constants seem to be consistent and no differences are noticeable between the results issued from measurements at resonance or out of resonance. Some improvements are needed to increase the accuracy of image freezing in the time domain. The present trigger process is probably responsible of the higher scatter of the two loss factors.

4 Improvement of the full-field measurement procedure

An improvement is currently in progress by using a 1024×1024 pixel high speed camera (12 bits monochromatic) to over sample the full-field measurements during several periods of excitation to obtain a nice temporal description of the deformation fields.
First, dynamic series of 100 to 300 images are taken with a frame rate of 6000 images per second. In regard to the used excitation frequencies that leads to the acquisition of 20 to 100 images per period of the harmonic response of the plate.
Then an interactive procedure is used to select the images of the considered dynamic series whose the phase maps relative to a static image remain unwrapped. The selected dynamic image becomes the reference image which phase fields provides the two "absolute" slope fields $\theta_x(x, y)$ and $\theta_x(x, y)$ relative to the undeformed case.
Due to the frame rate, the deformations of the plate between two successive acquisition times remain small so that the incremental series of phase maps obtained from the difference between two consecutive images remain unwrapped. These lead to the sets of the incremental maps of the slope field corresponding to the times of image sampling. Cumulative summations of these incremental slope fields, with respect to the reference slope ones provide the two sets of the "absolute" slope fields relative to the static case and corresponding to the times of the sampling rate.

One advantage of this procedure consists in setting up the excitation level in order to maximize the signal to noise ration although the unwrapping process of the phase maps is avoided.
Finally a least mean square regression is computed point by point through the sets of slope fields which leads to the extraction of the real and imaginary parts of the slope fields of the vibrating plate. It must be pointed out that no modal scheme is used for this determination, so the method works whatever the excitation frequency is close or not to a resonance. As mentionned in section 3.2, deflection and curvature fields are respectively issued from numerical integration and differentiation of polynomial fittings of the slope fields.
It must be pointed out that no modal scheme is used for this determination, so the method works whatever the excitation frequency is close or not to a resonance.

Figure 2 shows an example of such deflection field detection on an acrylic plate which was excited very close to its third mode frequency. For the sake of comparison, Fig. 3 shows the computed harmonic response in the same conditions provided by a standard FE code.The FE model of the plate is built using rectangular shell elements with four nodes and six degrees of freedom per nodes.

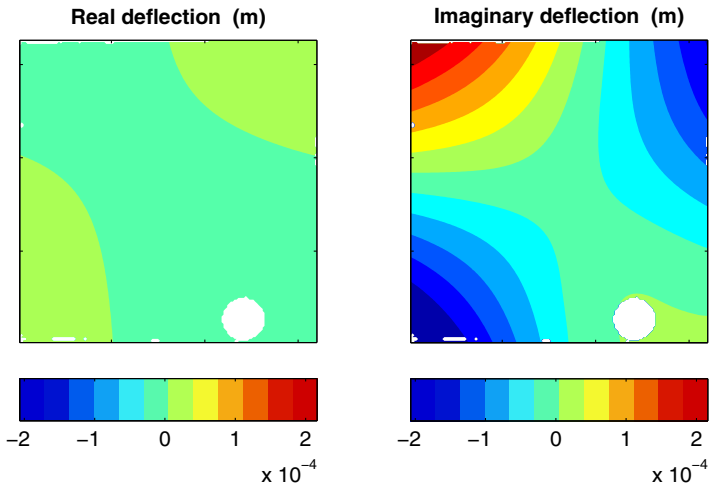

Fig. 2. Measured harmonic response on the resonance of the 3^{rd} mode ($83.3Hz$)

5 Conclusion

Previous studies have shown the principle of the Virtual Fields Method applied to vibrating plates and demonstrate the experimental feasibility. Some previous tests have proved the method greatly minimize the parasitic effects due to experimental conditions. This property obviously deserves a major attention since it offers a great interest for the material damping identification. This last study introduces an important way of improvement of the experimental part in order to increase the accuracy of the identification of the damping properties .

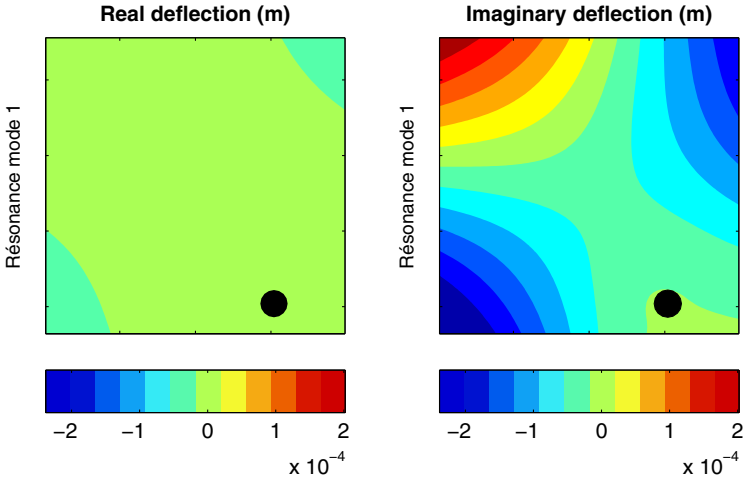

Fig. 3. FE simulated harmonic response on the resonance of the 3^{rd} mode

References

1. M. Grédiac, P.A. Paris, Journal of Sound and Vibration **193**(3), 401 (1996)
2. A. Giraudeau, F. Pierron, Journal of Sound and Vibration **284**(3-5), 757 (2005)
3. A. Giraudeau, F. Pierron, B. Guo, Journal of Sound and Vibration **329**(10), 1653 (2010)
4. E. Toussaint, M. Grédiac, F. Pierron, International Journal for Mechanical Sciences **48**(3), 256 (2006)
5. M. Grédiac, E. Toussaint, F. Pierron, International Journal of Solids and Structures **40**(10), 2401 (2003)
6. S. Avril, M. Grédiac, F. Pierron, Computational Mechanics **34**(6), 439 (2004)
7. Y. Surrel, *Deflectometry: a Simple and Efficient Non interoferometric Method for Slope Measurement*, in *SEM Annual Congress on Experimental Mechanics* (Society for Experimental Mechanics, 2004), 7-10 June in Costa Mesa, California, USA
8. A. Giraudeau, B. Guo, F. Pierron, Experimental Mechanics **46**(6), 777 (2006)
9. T. Pritz, Journal of Sound and Vibration **306**, 790 (2007)